

EUROPEAN ORGANIZATION FOR NUCLEAR RESEARCH
CERN - SPS DIVISION

CERN LIBRARIES, GENEVA



CM-P00063519

CERN SPS/87-32 (EMA)

LHC Note No 62

DESIGN OF A HIGH-FIELD TWIN APERTURE SUPERCONDUCTING DIPOLE MODEL

D. Leroy, R. Perin, G. de Rijk, W. Thomi

(Paper presented at the
10th International Conference on Magnet Technology,
Boston, Mass. 23-26 September, 1987)

(0703B)

Prévessin, 14th September 1987

DESIGN OF A HIGH-FIELD TWIN APERTURE SUPERCONDUCTING DIPOLE MODEL

D. Leroy, R. Perin, G. de Rijk, W. Thomi
 European Organization for Nuclear Research (CERN)
 1211 GENEVE 23 (Switzerland)

Abstract

In the framework of a Large Hadron Collider project in the LEP tunnel, considered as the natural long term extension of the CERN facilities, a development programme on high field superconducting dipoles is pursued at CERN. An initial design of a twin aperture superconducting dipole model is reported. It is a one meter long model using a NbTi superconducting cable at 2 K and designed for a central field of 9 to 10 T. The cable and the coil configuration, the magnetic field calculations and the mechanical concept are presented.

Introduction

Design, construction and tests on models are crucial to demonstrate the feasibility of the Large Hadron Collider (LHC) [1] to be installed in the tunnel of the CERN LEP machine. The design of the dipole magnets for the LHC is based upon the "two-in-one" concept, originally proposed and tested at Brookhaven National Laboratory for fields up to ~ 5 T. Following this concept, the dipole magnets of the two rings have a common magnetic circuit (Fig. 5) and are located in one cryostat. This solution is economical in space and cost and allows the installation of very high field magnets in the restricted space available in the LEP tunnel above the LEP machine components. As the attainable beam energy in the machine is proportional to the dipolar magnetic field, it is important to reach magnetic fields as high as possible. The envisaged field level for the LHC machine is in the range of 8 to 10 T. Two major lines of development are followed for the construction of models of high field magnets: 1) using Nb₃Sn superconducting cables at 4.5 K, 2) using NbTi alloy superconducting cables at 2 K.

Dipole models with one single aperture are now under construction following the two technology lines. Their basic design concepts and their status may be found in references [2, 3].

The models discussed in this report are one meter long twin aperture dipoles. They employ NbTi alloy superconducting cables at 2 K but, apart from the coils, the mechanical design concepts are equally valid for magnets using Nb₃Sn cables. A role of the models is to test the various components and procedures of fabrication in order to obtain the best performances at lowest costs. Possible variants in the design are mentioned.

Coils and conductors

The coils consist of two layers, each with a different high aspect ratio superconducting cable made of NbTi composites operating at 2 K. In each layer, the conductors are grouped into blocks and so distributed as to obtain a good field homogeneity (Fig. 1).

Provided that the problems related to the fabrication and winding of high aspect ratio cables can be solved, a two layer magnet appears a simple and economical solution. To obtain a 10 T nominal induction (B₀) with superconducting cables of reasonable width (17 mm), the two layers have a graded current density, though carrying the same current [3].

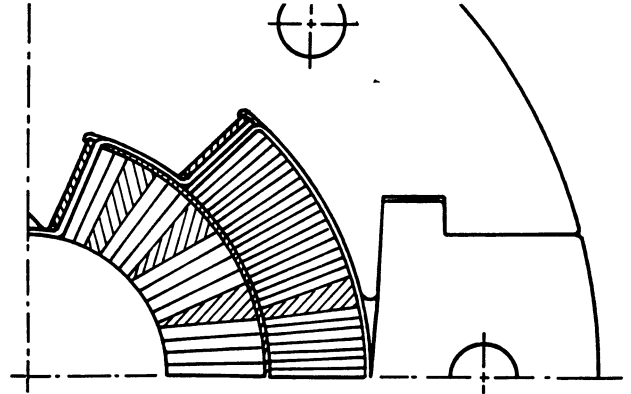


Fig. 1 - Conductor distribution in coils

The design characteristics of the two cables for the twin aperture dipole are summarized in table 1. The cable of the outer layer employs the strands developed for HERA. A cable of 40 strands has been fabricated and has a critical current of 19.0 kA at 8 T, 2 K (Fig. 2).

	Cable 1 inner layer	Cable 2 outer layer
Strand diameter (mm)	1.29	0.84
Cu/Sc ratio	1.6	1.8
Number of strands	26	40
Cable dimensions (mm ²)	2.06/2.50x17.0	1.3/1.67x17.0
Critical current (kA)	14 at 11 T	15.5 at 9 T

Table 1 - Characteristics of the two NbTi cables

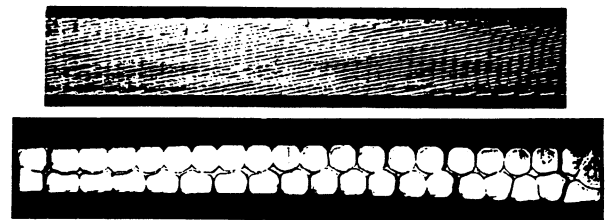


Fig. 2 - Picture of a 40 strand cable for the outer layer.

The design characteristics of the cable for the inner layer are based upon a current density of 1300 A/mm² at 11 T and 2 K, allowing for a copper to superconductor ratio of 1.6. At present it seems difficult to obtain the specified current density in strands of 1.29 mm Ø, although the optimization procedure has not yet been completed. The results obtained with the first prototype of the cable for the inner layer would imply a quenching field of 9.9 T (Fig. 3). The specified high current density could be attained in strands of 0.5 mm Ø. This implies multi-stage cables which have to be tested under a high compressive load (140 MPa).

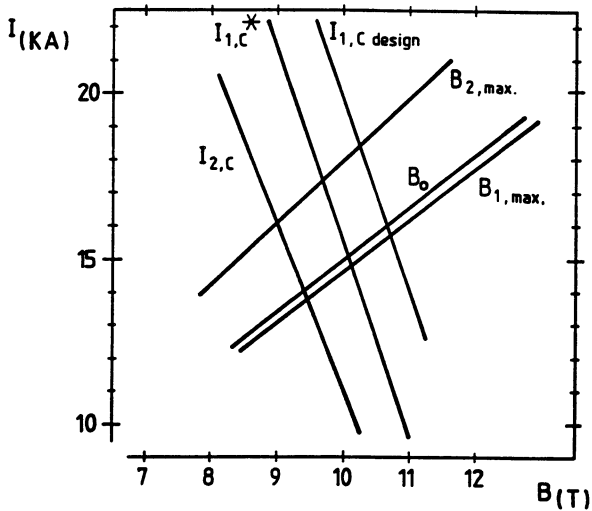


Fig. 3 - Load line and critical currents of the twin aperture model. $B_{1,max}$, $B_{2,max}$: inner and outer layer maximum field. $I_{1,C}^*$, $I_{2,C}$: obtained critical current in cables 1, 2

The mechanical stability of the cables is of great importance for the fabrication of the cable and the winding of the coil. Up to now mechanical stability has been obtained in the cable for the outer layer (40 strands of 0.84 mm \emptyset) by soldering, whereas tests have shown that a cable made of 36 strands of 0.93 mm could be fabricated and handled without solder. It is foreseen to use soldered cables for the first model.

The parameters of the twin aperture dipole are reported in Table 2.

Nominal field B_0 (2 K)	10	T
Operation current	15000	A
Turns per beam channel	1st layer	2 x 13
	2nd layer	2 x 24
Peak field in winding (T)	1st layer	10.2
	2nd layer	8.4
Overall current density in compressed and insulated cable (A/mm^2)	1st layer	357.5
	2nd layer	532.9
Operational current density (J_0) in NbTi at 2 K (A/mm^2)	1st layer	1150
	2nd layer	1900
J_0/J_c at 2 K	1st layer	0.77
	2nd layer	0.87
Coil inner diameter	50	mm
Coil outer diameter	120.2	mm
Distance between aperture axes	180	mm
Collars outer dimension	380	mm
Iron outer diameter	540	mm
Stor. energy for both channels combined	684	kJ/m
Self-inductance per single dipole	3.134	mH/m
Mutual inductance between dipoles	7.08	μ H/m
Resultant of magnetic forces in the first coil quadrant		
$\sum F_x$	=	227.6 t/m
$\sum F_y$, 1st layer	=	- 23.4 t/m
$\sum F_y$, 2nd layer	=	- 98.0 t/m

Table 2 - Dipole parameters at 2 K

As may be seen in Table 2 the safety margin is low for the outer layer cable which needs more copper than the inner layer cable for protection in case of a quench. The critical current density in the NbTi alloy is now assumed to be 2500 A/mm^2 at 5 T and 4.2 K, but current densities up to 3000 A/mm^2 have already been obtained on samples.

These high field magnets, employing 2 layers of windings operate at a high current, ~ 15 kA. This high current has consequences on :

- The by-pass diodes, which are required to have a high thermal capacity.
- The amount of copper to protect the bus bars.
- The losses in the superconducting cables during the charge and discharge of the machine.

Appropriate tests will be conducted to qualify these points.

4. Field quality

The multipole field components are defined by $B_y + iB_x = B_0 \sum (b_n + ia_n) (Z/R_r)^{n-1}$ with $n = 1, \dots, \infty$ and : B_0 = magnitude of the dipole field ; $Z = x + iy$; b_n , a_n = normal, skew multipole coefficient, $R_r = 1$ cm = reference radius. The conductors are distributed (Fig. 1) in the coils of a single dipole such that at low field the 6-, 10-, 14-, 18- pole components are minimum. Their values are given in Table 3.

2n	6	10	14	18	22
$\epsilon_n = B_n/B_0$	2.7×10^{-7}	3.9×10^{-7}	1.3×10^{-5}	2.4×10^{-6}	4.9×10^{-7}

Table 3 - Multipoles due to conductor distribution in the coils of a single dipole

The inner radius of the iron has been chosen as a compromise between field enhancement and saturation effects at high fields. The introduction of the individual dipoles in the "two-in-one" geometry creates additional multipole components, especially a quadrupole component. In the calculated configuration, there is no dipole field amplification caused by the proximity of the magnets. This is due to the relative dimensions of the iron yoke and the inter-beam distance.

Variations of the multipolar field content during the excitation originate from persistent currents in the superconductor, iron saturation and coil deformation under electromagnetic forces. Only the effects of the iron configuration at low and high field are discussed here. Multipolar coefficients have been calculated with the iron shapes shown in Fig. 4. The results are presented in Table 4.

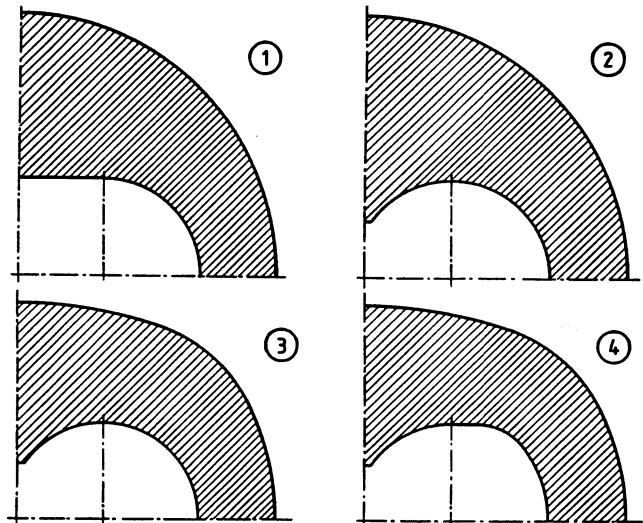


Fig. 4 - (1) Round iron yoke. (2) Round iron yoke descending between the two magnets. (3) Oval iron yoke descending between the two magnets. (4) Oval iron yoke, descending, shaped inner profile of the iron.

Iron Shape	(1)	(2)	(3)	(4)
B_0 at $I=15230A(T)$	10.12	10.22	10.16	10.10
Ampere-turn loss by iron saturation	1.58%	1.51%	2.09 %	2.04%
b_2 (1 T)	18.6	-1.39	-1.38	-14.95
b_2 (10T)	11.26	-3.50	-7.75	-17.53
b_2 (10T) - b_2 (1T)	-7.34	-2.11	-6.37	- 2.58
b_3 (1 T)	0.15	0.88	0.88	0.43
b_3 (10T)	1.72	2.03	1.82	1.53
b_3 (10T) - b_3 (1T)	1.57	1.15	0.94	1.1

Table 4 - Effect of the iron geometry on the multipolar coefficients at $R_r = 1$ cm in 10^{-4} units

The quoted values of b_2 and b_3 at 1 T are introduced by the "two-in-one" configuration. As it can be seen by the change of sign of $b_2(1 T)$ between the shapes (1) and (2), there exists an optimal height for the iron insert at which $b_2(1 T) = 0$. This quadrupolar component could also be compensated by introducing a left-right asymmetry in the coils. As an example, a wedge of $2 \times 0.67^\circ$ placed in the mid plane of the central coil layers creates a quadrupolar coefficient $b_2 = 19.5 \times 10^{-4}$. Moreover, the descending iron or the shaping of the inner profile of the iron reduces the saturation effect on the quadrupolar coefficient. Even if the oval shapes of the iron are less demanding in space, the 1 m long models will be constructed with a round iron yoke because of the simpler construction.

The coupling coefficient between the two magnets varies with the saturation as indicated in table 5.

B(T)	L(mH/m)	M(μ H/m)	k(%)
1.4	3.134	7.08	0.226
10.1	2.89	153.4	5.3

Table 5 - Self, mutual inductance and coupling coefficient $k = M/L$

The effect of a difference of 1 % in the excitation of one of the two magnets assembled in the "two-in-one" construction has been computed to result in the other magnet to a variation of 1.8×10^{-5} in the dipolar and 1×10^{-5} in the quadrupolar coefficients at 0.5 T.

Mechanical structure of the twin aperture dipole

The mechanical structure is conceived for an 11 T central field. As shown in Fig. 5, the coil support structure is formed by :

- A twin collar, made from an aluminium alloy, in which the coils are assembled and moderately prestressed at room temperature.
- An iron yoke, split in two parts at the vertical symmetry plane of the twin aperture magnet. The two iron inserts between collars and yoke serve to reduce the quadrupole component in the twin aperture dipole.
- A stainless steel or aluminium alloy shrinking cylinder around the yoke.

In view of keeping the volume of superfluid He in the magnet as small as possible and to reduce the cooling time from 4.2 K to 2 K, the interspaces between the iron laminations are filled with a

material of high thermal contraction, so that the laminated steel yoke has a global longitudinal thermal contraction equivalent to stainless steel. End plates are welded onto the shrinking cylinder and take most of the axial magnetic force on the coil ends (853 kN for the 2 magnets).

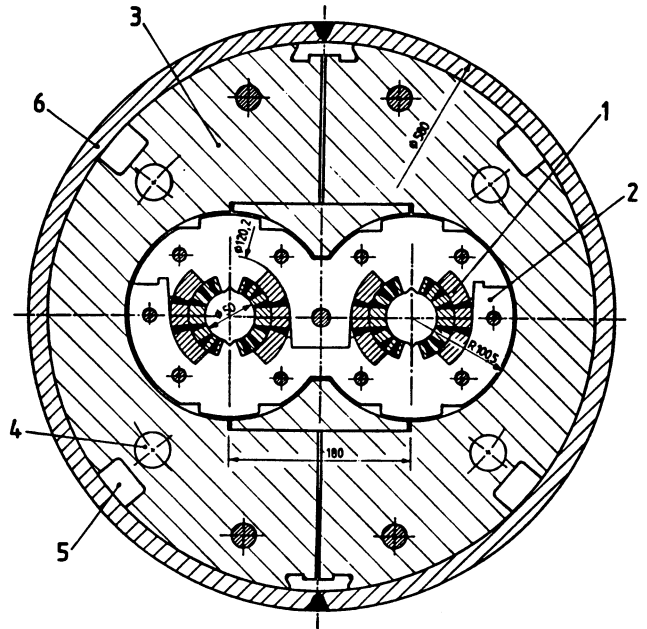


Fig. 5 - Cross-section of a twin aperture dipole. 1) Coils, 2) Collars, 3) Iron yoke, 4) He duct, 5) Bus-bar slot, 6) Shrinking cylinder.

The two parts of the yoke are separated by a gap at room temperature and so adjusted that after cool-down, the collars and the yoke are in contact, and a compression is produced on the mating faces of the yoke parts. If the compressive force on the mating yoke faces is equal or larger than the maximum horizontal resultant of the magnetic forces, the gap stays closed in all operating conditions of the magnet. The resulting mechanical structure is very rigid and has therefore small displacements under the large magnetic forces. The possibility to have, after cool-down, a compressive force on the mating faces of the half-yokes and a closed contact between the collars and the yoke depends on the relative dimensions of the components of the structure and the choice of materials. Moreover, when the inward displacement of the iron in the horizontal direction is larger than the corresponding shrinkage of the collared coils during the cool-down, an additional prestress is introduced on the coils at low temperature. The difference between the required stressing of the coils at operating conditions and the loading produced by the cool-down of the structure determines the prestress which has to be provided at room temperature by coil collaring.

At an 11 T magnetic field, the horizontal resultant of the forces in a quadrant of a magnet is 2860 N/mm. When the iron is tightly closed at low temperature, the parts of the horizontal magnetic force taken by the collars and by the discharge of the two mating surfaces of the yoke will depend on the relative stiffness of the collars and the iron. Calculations indicate that 30 % of the horizontal force can be taken by the collars with a displacement of the contact point between the collars and the iron not larger than 0.08 mm while the center of the magnet moves outward by 0.04 mm. The external cylinder could then be designed to support 70 % of the magnetic force.

	Inner layer		Outer layer	
	$\theta=0^\circ$	$\theta=74^\circ$	$\theta=0^\circ$	$\theta=47.7^\circ$
$S_\theta (r_{in})$	- 47	+ 70	- 55	+ 35
$S_\theta (r_{out})$	- 25	+ 10	- 35	+ 10

Table 6 - Azimuthal S_θ stresses due to magnetic forces alone (in MPa)

The stresses in the coils due to the electromagnetic forces applied in such a structure are shown in table 6. They vary with the radius. It can be seen that the electromagnetic forces increase the compression in the median plane and discharge the coil at the upper angle of the layer.

Tables 7.a and 7.b show the calculated stresses at room temperature and at low temperature for $B = 0$ and $B = 11$ T in the coils and in the shrinking cylinder. The stresses in the coils at room temperature represent the minimum compression necessary to keep the contact between the collars and the coils at the upper angle of the layers and ensure that no tensile stresses occur in the coils at high field. In this calculation, there is no prestressing in the coils due to the cooldown of the shrinking cylinder which is stressed so that the contact between the collars and the iron is just maintained in the horizontal direction and the necessary force on the yoke mating faces is attained during cool-down. The stresses in the coils are increased at low temperature only by the differential displacement between coils and collars.

	Inner layer		Outer layer	
	$\theta=0^\circ$	$\theta=74^\circ$	$\theta=0^\circ$	$\theta=47.7^\circ$
Minimum prestress room temperature (MPa)	- 55	- 55	- 35	- 35
Stresses at 2 K $B = 0$	- 73	- 73	- 42	- 42
Stresses at 2 K r_i $B = 11.2$ T r_o	-120	- 3	- 97	- 7
	- 98	- 63	- 77	- 32

Table 7.a - Azimuthal stresses in the coils

Material	Shrinking cylinder	
	Al Mg 4.5	St. Steel
Thickness (mm)	18	12
Prestress at room temperature (MPa)	10	286
Stresses at 2 K $B = 0$ (MPa)	120	166
Stresses at 2 K $B=11$ T (MPa)	120	166

Table 7.b - Azimuthal stresses in shrinking cylinder

With the dimensions of the various components of the twin aperture magnet, a prestress is required at room temperature in the external cylinder in order to obtain the compressive forces on the mating faces and the contact between collars and yoke (Table 7b). The

gap between the two half-yokes is ~ 0.8 mm at room temperature. The room temperature stresses which have to be settled in the case of a stainless steel cylinder induce high stresses in the coils, which will disappear at cold conditions. These stresses could be avoided by the insertion, between the half-yokes, of a support having a high thermal contraction so that the closing of the gap is not prevented. In the case of an Al alloy cylinder, sliding perfectly on the yoke in all directions, the prestress at room temperature would be 60 MPa. By fixing the cylinder to the two ends of the yoke, which has a longitudinal thermal contraction of $2.8 \cdot 10^{-3}$, one can take benefit of the longitudinal stresses to increase the hoop stresses during cool-down. The longitudinal stresses in the Al alloy cylinder amount to 150 MPa, which gives an additional 50 MPa in the azimuthal direction of the cylinder. Comparing the two possible materials for the shrinking cylinder, Al alloy (AlMg4.5) is limited by the yield strength of the welded part at 2 K ($\sigma_{0.2} = 200$ MPa) whereas 304N stainless steel is limited at room temperature at 300 MPa. For the mechanical structure of the magnets, Al alloy is preferable but the welding method and the connections at the ends of the magnet have to be carefully studied to use the Al alloy shrinking cylinder as the outer wall of the cryostat at 2 K. It is intended to construct different models using different materials.

The largest stresses occur in the median plane at the inner radius of the inner layer. Given the relative dimensions of collars and iron and the wanted precompression on the iron mating faces, the inward displacement of the iron can be larger than the displacement of the collars at cool-down only if an adequate tensile prestress exists in the shrinking cylinder at room temperature. With respect to the values of table 7.b, an increase of prestress in the Al alloy shrinking cylinder by 30 MPa would decrease the compressive stress by 10 MPa in the median plane, but increase it by 18 MPa at the upper angle of the inner layer. The total compressive stress in the median plane could then be reduced by 28 MPa at 11 T.

In case of a quench in a 10 m long magnet, the temperature of the coil should not exceed 300 K when heaters are activated to distribute the quench all over the two layers. The resulting thermal stresses in the coils have been estimated at 40 MPa. Because the magnet is discharging when these thermal losses occur, the azimuthal compression in the median plane of the coils should not exceed 140 MPa.

Acknowledgements

The work reported in this paper benefited of the discussions and contributions of many colleagues from CERN and other Institutions, in particular CEA (France). M. Bona (CERN TIS-MC) deserves a particular acknowledgement for setting up the finite element calculations of mechanical structures. The continuous support and encouragement by the CERN Direction and fruitful discussions with the colleagues of the LHC Study Group and Cryogenics Group are also gratefully acknowledged.

References

- [1] The Large Hadron Collider in the LEP tunnel, edited by G. Brianti and K. Hübner, CERN 87-05
- [2] R. Perin, Progress on the Superconducting Magnets for the Large Hadron Collider, presented at this Conference.
- [3] D. Hagedorn, D. Leroy, R. Perin, Towards the Development of high Field Superconducting Magnets for a Hadron Collider in the LEP Tunnel, Proc. 9th Int. Conf. on Magnet Technology, p. 86-91, Zürich, 1985, LHC Note 31.